British Journal of Pharmacology

DOI:10.1111/j.1476-5381.2011.01627.x
www.brjpharmacol.org

RESEARCH PAPER

Long-term treatment with ivabradine in post-myocardial infarcted rats counteracts f-channel overexpression

S Suffredini[1], F Stillitano[1], L Comini[2], M Bouly[3], S Brogioni[1], C Ceconi[4], R Ferrari[4], A Mugelli[1,5] and E Cerbai[1,5]

[1]*Center of Molecular Medicine (C.I.M.M.B.A.), Florence, Italy,* [2]*Fondazione S. Maugeri, Gussago (BS), Italy,* [3]*IRIS, Servier, France,* [4]*Department of Cardiology and LTTA Centre, University Hospital of Ferrara and Salvatore Maugeri Foundation, IRCCS, Lumezzane, Italy, and* [5]*Department of Pharmacology, University of Florence, Florence, Italy*

Correspondence
Professor Elisabetta Cerbai, Department of Pharmacology, University of Florence, Viale G. Pieraccini 6 50139, Florence, Italy. E-mail: elisabetta.cerbai@unifi.it

Keywords
electrophysiological remodelling; f-current; heart rate; ivabradine; post-MI rat; hyperpolarization-activated cyclic nucleotide-gated channels

Received
30 December 2010
Revised
21 July 2011
Accepted
26 July 2011

BACKGROUND AND PURPOSE

Recent clinical data suggest beneficial effects of ivabradine, a specific heart rate (HR)-lowering drug, in heart failure patients. However, the mechanisms responsible for these effects have not been completely clarified. Thus, we investigated functional/molecular changes in I_f, the specific target of ivabradine, in the failing atrial and ventricular myocytes where this current is up-regulated as a consequence of maladaptive remodelling.

EXPERIMENTAL APPROACH

We investigated the effects of ivabradine (IVA; 10 mg·kg^{-1}·day^{-1} for 90 days) on electrophysiological remodelling in left atrial (LA), left ventricular (LV) and right ventricular (RV) myocytes from post-mycardial infarcted (MI) rats, with sham-operated (sham or sham + IVA) rats as controls. I_f current was measured by patch-clamp; hyperpolarization-activated cyclic nucleotide-gated (HCN) channel isoforms and microRNA (miRNA-1 and miR-133) expression were evaluated by reverse transcription quantitative PCR.

KEY RESULTS

Maximal specific conductance of I_f was increased in MI, versus sham, in LV ($P < 0.01$) and LA myocytes ($P < 0.05$). Ivabradine reduced HR in both MI and sham rats ($P < 0.05$). In MI + IVA, I_f overexpression was attenuated and *HCN4* transcription reduced by 66% and 54% in LV and RV tissue, respectively, versus MI rats (all $P < 0.05$). miR-1 and miR-133, which modulate post-transcriptional expression of *HCN2* and *HCN4* genes, were significantly increased in myocytes from MI + IVA.

CONCLUSION AND IMPLICATION

The beneficial effects of ivabradine may be due to the reversal of electrophysiological cardiac remodelling in post-MI rats by reduction of functional overexpression of HCN channels. This is attributable to transcriptional and post-transcriptional mechanisms.

Abbreviations

HCN, hyperpolarization-activated cyclic nucleotide-gated channels; HR, heart rate; LA, left atrial myocytes; LV, left ventricular myocytes; MI, myocardial infarction; RV, right ventricular myocytes

Introduction

Ivabradine is a selective inhibitor of the hyperpolarization-activated, cyclic nucleotide gated pacemaker current I_f, a mixed Na^+/K^+ inward current activated by hyperpolarization, which plays a physiological role in controlling the heart rate (HR) and sensing its autonomic control in the sinus node (DiFrancesco, 2006; Liu *et al.*, 2007). Recent clinical data obtained in heart failure (HF) patients treated with ivabradine (the systolic heart failure treatment with I_f inhibitor ivabradine trial (SHIfT), Böhm *et al.*, 2010; Swedberg *et al.*, 2010) show that administration of ivabradine resulted in a

© 2011 The Authors
British Journal of Pharmacology © 2011 The British Pharmacological Society

significant reduction in cardiovascular death or hospital admission for worsening of HF. One potentially beneficial mechanism of ivabradine may consist of its ability to reduce ventricular work through a reduction in HR, thus reversing the remodelling processes.

Consistent with this hypothesis, we have recently demonstrated that HR reduction with ivabradine optimizes energy consumption and has a favourable impact on ventricular electrophysiological and structural remodelling in a rat model of chronic post-myocardial infarction (MI) (Ceconi *et al.*, 2011). To further support a causal relationship between the bradycardic effect of ivabradine and global remodelling in MI, a significant correlation between HR and cardiac phenotype was observed (Ceconi *et al.*, 2011). However, as pointed out in the accompanying comment to the SHI_fT (Teerlink, 2010), the mechanisms for the beneficial effects of ivabradine in HF patients remain to be fully explored. A direct effect of ivabradine on I_f in non-pacemaker cells may be implicated (Teerlink, 2010), because it has been clearly documented that I_f is up-regulated in atrial and ventricular myocytes from HF patients (Cerbai *et al.*, 1997; 2001; Hoppe and Beuckelmann, 1998; Stillitano *et al.*, 2008). Studies in rats have demonstrated that I_f density is significantly higher in left ventricular (LV) myocytes isolated from severely hypertrophied or failing hearts compared with control rat hearts (Cerbai *et al.*, 1996; Fernandez-Velasco *et al.*, 2003; Sartiani *et al.*, 2006). However, the consequence of chronic channel blockade by ivabradine on disease-induced I_f up-regulation in non-pacemaker cells has not been reported so far. Notably, in mouse sinoatrial node, chronic HR reduction with ivabradine has been shown to up-regulate mRNA levels of *HCNs* (the genes coding for the alpha subunit of the I_f channels), a rebound phenomenon interpreted as an adaptive consequence of ivabradine treatment (Leoni *et al.*, 2005). Thus, direct (e.g. due to chronic channel blockade) and indirect effects (e.g. impact of HR reduction on the global remodelling) (Ceconi *et al.*, 2011) may act in opposite directions with unforeseen results.

The present study aimed to gain further insight into the effects of long-term administration of ivabradine in a rat model of post-MI remodelling by focusing on electrophysiological and molecular expression of I_f, that is, the specific target of the drug. Taking into account the regional differences in the functional and molecular expression of f-channels (Sartiani *et al.*, 2006), I_f and HCNs were assessed in LV, left atrial (LA) and right ventricular (RV) myocytes from infarcted rats treated with either ivabradine or vehicle for 3 months; sham-operated animals were used as controls. Our results show that long-term treatment of infarcted rats with the I_f inhibitor ivabradine, contrary to what was reported in the sinoatrial node (Leoni *et al.*, 2005), partially reverses electrophysiological cardiac remodelling through a decrease in functional and molecular *HCN2* and *HCN4* overexpression in ventricular and atrial cardiomyocytes.

Methods

Study design

All animal care and experimental procedures complied with the *Guide for Care and Use of Laboratory Animals* (NIH publication no. 85–23, revised 1996). Male anaesthetized (Zoletil + xylazine) Wistar rats aged 8–10 weeks and weighing 220–270 g underwent left anterior descending (LAD) coronary artery ligation, which was completely occluded by a 6-0 suture between the pulmonary artery outflow tract and the LA. One week after LAD ligation, the surviving post-MI animals (50%) were allocated into two homogeneous groups on the basis of LV diastolic dimension and fractional shortening assessed by echocardiography, as previously described (Ceconi *et al.*, 2011). Each group received either vehicle (MI group; $n = 15$) or ivabradine in drinking water at the dose of 10 mg kg^{-1}·day^{-1} (MI + IVA group; $n = 15$) for 90 days. The study duration of 90 days and ivabradine dosage were selected according to the time required to observe biochemical and cellular remodelling, on the basis of comparison with other studies in the post-MI model (Mulder *et al.*, 2004; Ceconi *et al.*, 2011). Due to technical reasons related to cell isolation procedure, some rats were used for electrophysiological (EP) studies and others allocated to molecular biology (MB) studies. In the MI and MI + IVA groups, eight rats were used for EP and seven for MB studies. Control sham-operated rats underwent the same procedure, except that the suture was tied loosely so as not to obstruct coronary artery flow; they received vehicle only or ivabradine for 3 months (sham: $n = 6$ for EP and $n = 6$ for MB studies; sham + IVA: $n = 6$ for EP and $n = 6$ for MB studies). For the sake of homogeneity, only free wall from the LV and RV was selected for both EP and MB experiments; the whole LA (not the RA) was used according to previous evidence of f-channel up-regulation and electrophysiological remodelling in human ischaemic cardiomyopathy (Stillitano *et al.*, 2008).

Myocyte isolation and electrophysiology

After the 3 month treatment period, rats were anaesthetized (pentothal, 30 mg kg^{-1}, i.p.) and were killed by guillotine. After thoracotomy, the heart was rapidly excised, mounted on a Langendorff apparatus, and perfused for 20 min with a low-calcium solution (LCS) prewarmed to 37°C and equilibrated with 100% O_2. The solution was then quickly changed to LCS plus 0.1% type II collagenase (Worthington Biochemical Corporation, Lakewood, CO, USA) and 0.1% albumin (Fatty Acid Free Fraction V, Sigma-Aldrich, St Louis, MO, USA) for 15–20 min. The ventricles and LA were excised, homogenized and stirred in LCS. Each supernatant was resuspended in fresh LCS and myocytes were purified by gravity sedimentation, and collected and stored in Tyrode solution containing 0.5 mM $CaCl_2$ and 4% penicillin/streptomycin solution.

Myocardial patch-clamp recordings were performed using protocols and equipment similar to previous reports (Cerbai *et al.*, 1996). The whole-cell configuration of the patch-clamp technique was used to record ionic currents in at least eight cells per group per parameter on an inverted microscope (Nikon Diaphot, Tokyo, Japan) with a patch amplifier (Axopatch-200B, Axon Instruments, Union City, CA, USA). Cells were superfused with normal Tyrode solution to measure membrane capacitance (C_m) and the inward rectifier current I_{K1}, or with Tyrode solution properly modified to measure the I_f current. The patch-clamped cell was superfused by means of a temperature-controlled microsuperfusor, allowing rapid changes in the solution bathing the cell. Temperature was maintained in the range of 36–37°C.

C_m was measured as described previously (Sartiani *et al.*, 2006). In LV cardiomyocytes, C_m was not significantly different in all groups, although a trend towards increase was observed in MI rats (sham 179 ± 18 pF, n = 12 (five rats); sham + IVA: 152 ± 19 pF, n = 7 (five rats); MI: 265 ± 39 pF, n = 21 (seven rats); MI + IVA 210 ± 9 pF, n = 22 (eight rats).

I_f was elicited by hyperpolarizing steps (–10 mV) ranging from –60 to –130 mV applied from a holding potential of –30 mV. The duration of pulses was progressively reduced with more positive voltage from 3200 ms (at –50 mV) to 1600 ms (at –140 mV). This was done to use steps that were as short as possible (given that kinetics become faster at more negative voltages), because cells tolerate poorly prolonged voltage steps. Fitting was carried out by using the Chebyshev fitting routine of the Clampfit program (pClamp vers. 9; first order exponential fit). Amplitude was automatically calculated as the difference between the value at the beginning of the hyperpolarizing step and the value extrapolated to the steady state. Boltzmann fitting of activation curves was evaluated by errors of variable parameters; only satisfactory curves were considered for the analysis (Sartiani *et al.*, 2006). I_{K1} was measured during application of a ramp protocol (–120 to +50 mV) as barium-sensitive current, after superfusing with 0.5 mM $BaCl_2$.

Solutions

LCS contained (in mM): NaCl 120, KCl 10, KH_2PO_4 1.2, $MgCl_2$ 1.2, D-glucose 10, taurine 20, HEPES 10 (pH 7.2 with NaOH). Normal Tyrode's solution (in mM): NaCl 140; KCl 5.4; $CaCl_2$ 1.8; $MgCl_2$ 1.2; D-glucose 10; HEPES 5 adjusted to pH 7.35 with NaOH. Modified Tyrode's solution for I_f (in mM): NaCl 140, KCl 25, $CaCl_2$ 1.8, $MgCl_2$ 1.2, $BaCl_2$ 2, $MnCl_2$ 2, 4-aminopyridine 0.5, D-glucose 10, HEPES 5, adjusted to pH 7.35 with NaOH. Internal solution (in mM): K-Aspartate 130; Na_2-ATP 5, $MgCl_2$ 2, $CaCl_2$ 5, EGTA 11, HEPES 10 adjusted to pH 7.2 with NaOH. The pipette junction potential (≈10 mV) between external and internal solution was not corrected.

Quantification of HCN2 and HCN4 transcripts

Immediately after death, the LV, LA and RV were excised from the heart; each sample was frozen in liquid nitrogen and was stored at –80°C. Total RNA was harvested from frozen tissue using a column-based extraction method (RNeasy Fibrous Tissue Mini Kit, Qiagen, Hilden, Germany). Expression of *HCN2* and *HCN4* transcripts in myocytes isolated from the LV, LA and RV was evaluated using quantitative reverse transcription PCR (qRT-PCR). First, strand cDNAs were synthesized at 48°C using TaqMan Reverse Transcription Reagents (N808-0234, Applied Biosystems, Foster City, CA, USA) in a 100 µL reaction mixture containing 2 µg RNA and 2.5 µM random hexamer primers. qPCR was performed using an ABI Prism 7500 Sequence Detection System with TaqMan gene expression assays ordered from Applied Biosystems to evaluate expression of *HCN2* (assay No. Rn01408575_gH) and *HCN4* (assay No. Rn00572232_m1). When evaluated by the same method, the gene *GAPDH* (assay no. 4352338E) showed stable expression in the LA, LV, and RV myocytes under all of the experimental conditions, and was therefore used as an internal control gene. Relative gene expression was determined using the $2^{-\Delta\Delta CT}$ method (Livak and Schmittgen, 2001).

Expression of miR-1, miR-133a and miR-133b

miRNA levels were determined by qRT-PCR. Briefly, RNAs from LV and LA tissue were isolated with the mirVana miRNA Isolation Kit (Ambion, Applied BioSystems, Monza, Italy). The kit includes organic extraction followed by immobilization of RNA on glass-fibre filters to purify either total RNA, or RNA enriched for small species, from cells or tissue samples. qRT-PCR was performed by using TaqMan MicroRNA Assays from Applied Biosystems, which use looped-primer RT-PCR (a new real-time quantification method) to accurately detect mature miRNAs. Each TaqMan MicroRNA Assay includes: miRNA-specific RT primers, miRNA-specific forward PCR primer, specific reverse PCR primer, and miRNA-specific TaqMan MGB probe. cDNA was generated from 150 ng total RNA. As an internal control, snRNA_U6 primers and probe (Applied Biosystems; #4395470) were used for RNA template normalization. The qPCR reactions were performed using TaqMan Gene Expression Master Mix (Applied BioSystems) in a 20 µL reaction volume containing 1 ng cDNA. All reactions were performed in triplicate and included a negative control. PCR reactions were carried out using an ABI Prism 7500 Sequence Detection System (Applied Biosystems). Cycling conditions were: 2 min at 50°C, 10 min at 95°C, and 40 cycles of 15 s at 95°C, and 1 min at 60°C. Relative quantification of miRNA levels was determined by the 7500 system software via the comparative method (ΔΔCT).

Statistical analysis

All data are presented as mean ± SEM. Student's t-test for paired data was used to compare individual HR measurements at 7 and 83 days. One-way ANOVA followed by a Tukey test was used to compare I_f; the statistics have been conducted by using both n = number of animals and n = number of cells, as indicated in the text. One-way ANOVA followed by a Tukey's test was used for qRT-PCR data between the three groups, with n representing the number of animals. Two-way ANOVA was used to compare I_f activation curves (n = number of rats). In all cases, where a parametric test was employed, the data conform to a standard distribution and the variances of the compared groups were comparable.

A χ^2 test was used to compare the occurrence of I_f in the RV among the three groups (n = number of cells). A P-value of less than 0.05 was considered statistically significant.

Results

Effect of ivabradine on HR

Individual HR values measured in MI and sham rats at the beginning (day 7) and end (day 83) of treatment with ivabradine or vehicle are reported in Figure 1; a significant decrease was observed in MI + IVA and sham + IVA groups when comparing values at day 7 and day 83 (Student's t-test, paired data), but not in MI or sham rats.

I_f properties in LV, LA and RV myocytes

Three months after ligation, maximal specific conductance of I_f was significantly increased in the post-MI rats versus sham

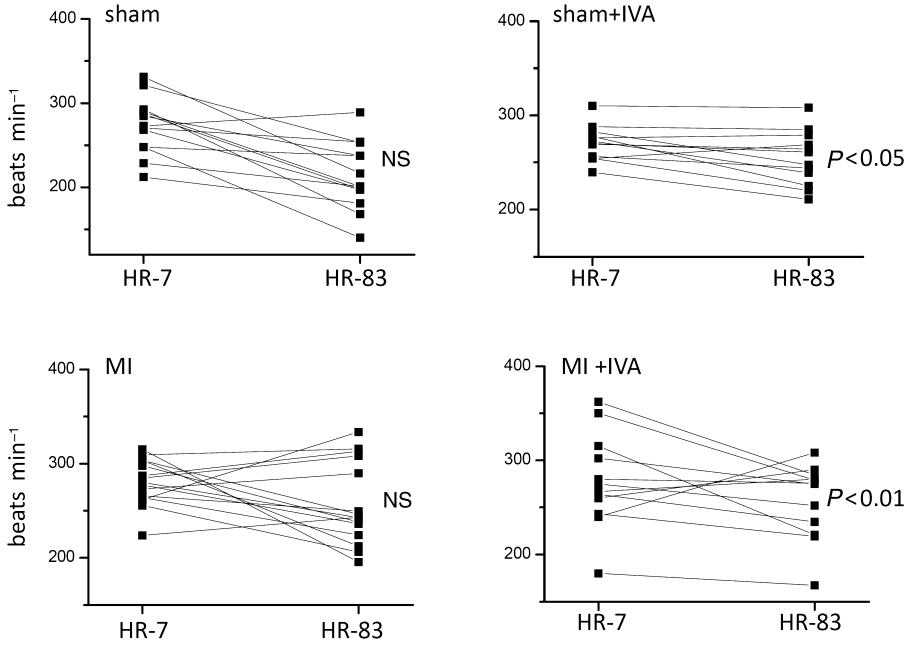

Figure 1

Individual heart rate measurements at the beginning (HR7) and end (HR83) of treatment with vehicle (left panels) or 10 mg·kg^{-1}·day^{-1} ivabradine in drinking water (n = 12 sham; n = 12 sham + IVA; n = 15 MI; n = 15 MI + IVA; P < 0.05 or P < 0.01, Student's t-test for paired data). MI, myocardial infarction.

in LV myocytes (64.7 ± 11.6 pS/pF n = 21 and 26.5 ± 6.3 pS/pF n = 12, MI vs. sham P < 0.01) and LA myocytes (66.0 ± 15.8 pS/pF n = 12 and 20.8 ± 4.4 pS/pF n = 12, MI vs. sham P < 0.05) with the n-value representing the number of cells. The same statistically significant difference was observed by averaging I_f values measured in individual hearts (thus, considering cells as replicates) and then performing statistics with the n-value representing the number of animals (LV: 62.6 ± 8.5 pS/pF, n = 7 vs. 23.5 ± 7.2 pS/pF, n = 5, P < 0.01; LA: 67.2 ± 11.4 pS/pF, n = 4 vs. 21.1 ± 5.8 pS/pF, n = 5, P < 0.05) (Figure 2A, B). Treatment with ivabradine (n = 8 rats) lowered f-current conductance in LV and LA myocytes by 30% (21 cells) and 28% (16 cells), respectively, although the difference did not reach statistical significance when comparing current density at individual voltages. Thus, in order to compare the curves over the whole range of step voltages used to elicit I_f, we applied two-way ANOVA; the effect of drug treatment was statistically significant (MI vs. MI + IVA) in LV and LA cells when performing statistics with the n-value representing either the number of animals (P < 0.01 for both) (Figure 2A, B) or the number of cells. This indicates that, in MI rats, treatment with ivabradine results in a uniform I_f loss-of-function in LV and LA cardiomyocytes with respect to untreated rats, as also suggested by similar voltage of half-maximal activation [sham: −106.9 ± 2.5 mV; MI: −113.6 ± 3.3 mV, MI + IVA: −107.1 ± 3.2 mV, non significant (NS) for all]. Figure 2C shows representative I_f recordings obtained in LV myocytes from sham, MI and MI + IVA rats. In order to assess whether ivabradine *per se* could affect current properties in basal conditions, I_f conductance was also measured in sham + IVA rats. In LV myocytes, I_f maximal conductance was 26.7 ± 4.1 pS/pF (n = 5 rats, 7 cells), not significantly different from the sham group.

Because of the low current conductance, I_f was detected in a minority of RV myocytes from sham rats; thus, in Figure 3, we report occurrence of I_f (i.e. the number of RV myocytes expressing a measurable I_f at −110 mV) rather than its density among all groups. The occurrence of I_f was 21% (4 out of 19 cells, 21 ± 4 pS/pF, n = 6 rats) in RV myocytes from sham rats and 64% (20 out of 31 cells; 49.5 ± 11.5 pS/pF, n = 8 rats) in RV myocytes from MI rats (P < 0.01 for I_f occurrence, χ^2 test, sham vs. MI rats). Treatment with ivabradine reduced the occurrence of I_f, which was detected in 32% (9 out of 28 cells; 33.3 ± 8.7 pS/pF, n = 8 rats) of the RV myocytes (P < 0.05 vs. MI rats, χ^2 test for occurrence of I_f). Although changes observed for I_f conductance in RV cells mirror those measured in LV and LA myocytes from the same groups, we did not perform a statistical comparison due to the difference in sample size among the groups.

Because the contribution of I_f to the diastolic phase is modulated by overlapping currents, namely the inward rectifier current, we measured I_{K1} density and reversal potential in the LV, LA and RV myocytes. No changes were observed in I_{K1} density or reverse potential (Table 1).

Transcript expression of HCN2 and HCN4 in LV, LA and RV myocytes

In order to investigate the molecular basis underlying up-regulation (MI) and down-regulation of I_f gain-of-function, we measured mRNA levels of the two main isoforms *HCN2* and *HCN4*, coding for f-channel alpha subunits. The results of qRT-PCR quantification in the LV, LA and RV tissue samples are shown in Figure 4. *HCN2* mRNA was significantly higher in the LV and LA of MI rats versus sham (both

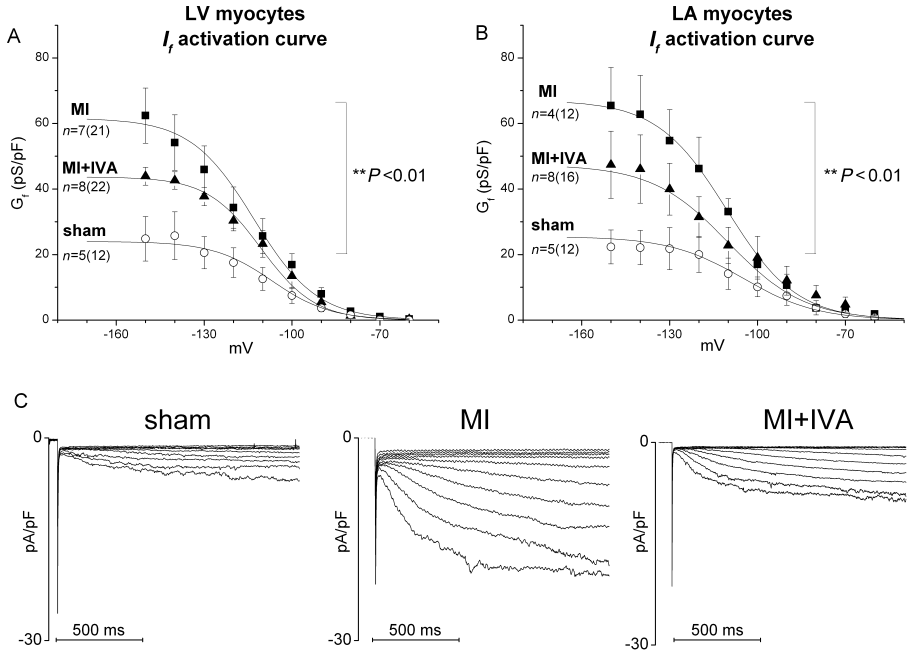

Figure 2

I_f activation curves for left ventricular (LV, A) and left atrial (LA, B) myocytes isolated from post-myocardial infarcted rats receiving ivabradine (10 mg·kg^{-1}· day^{-1} in drinking water) for 3 months (MI + IVA), post-myocardial infarcted (MI) rats and sham-operated animals receiving vehicle for 3 months. (C) Typical I_f recordings obtained in LV myocytes from sham, MI and MI + IVA rats. Number of animals and cells (in parenthesis) are shown in the figure. **P < 0.01, two-way ANOVA for activation curves (sham, MI and MI + IVA).

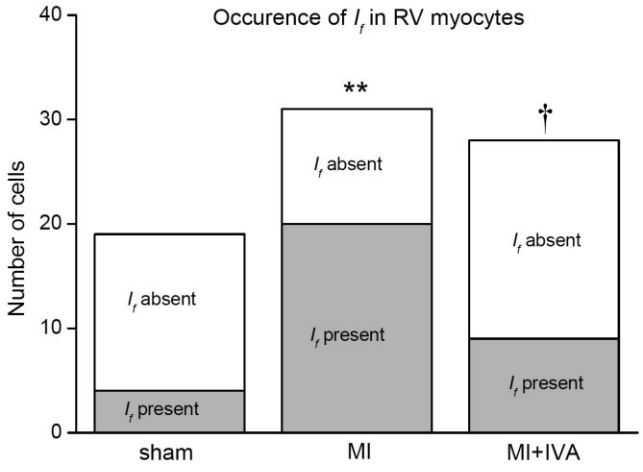

Figure 3

Occurrence of I_f in right ventricular (RV) myocytes isolated from post-myocardial infarcted rats receiving ivabradine (10 mg·kg^{-1}·day^{-1} in drinking water) (MI + IVA), post-myocardial infarcted rats (MI), and sham-operated animals receiving vehicle for 3 months. Each column represents the number of cells; 6 sham, 8 MI and 8 MI + IVA rats were used for experiments. **P < 0.01 MI versus sham, $^{\dagger}P$ < 0.05 MI + IVA versus MI, for expression of I_f, χ^2 test.

P < 0.01), as was *HCN4* mRNA in the LV (P < 0.05), LA (P < 0.01) and RV (P < 0.05). *HCN2* overexpression predominated in the LA, whereas *HCN4* overexpression predominated in the LV and RV (Figure 4). Treatment with ivabradine down-regulated this overexpression, although the effect was more evident in the ventricles than in the LA. *HCN2* expression was decreased by 26% in the LV (NS vs. MI); *HCN4* expression was decreased by 66%, and 54% in the LV and RV, respectively (P < 0.05 vs. MI). In the LV, *HCN2* and *HCN4* mRNA levels measured in MI + IVA group returned to values similar to those of the sham baseline (not significant vs. sham). In sham + IVA rats (n = 6), no decrease in *HCN2* or *HCN4* expression was observed. mRNA levels were 1.7 ± 1.2 (LA), 1.1 ± 0.4 (RV) and 1.5 ± 0.3 (LV) for *HCN2*, and 2.0 ± 0.6 (LA), 1.5 ± 0.5 (RV) and 1.5 ± 0.7 (LV) for *HCN4*. In the LA, the *HCN2* and *HCN4* mRNA levels were slightly decreased in MI+IVA versus MI (38% and 15%, respectively) and remained significantly higher than sham (Figure 4), thus suggesting that post-transcriptional mechanisms may also contribute to the reduction in current density observed in patch-clamp studies. This result prompted us to evaluate factors affecting HCN post-transcriptionally.

Transcript expression of miRNA in atrial and ventricular tissue

Recent evidence demonstrates that down-regulation of muscle-specific miRNA, miR-1 and miR-133, contributes to *HCN2* and *HCN4* overexpression in ventricular hypertrophy (Luo *et al.*, 2008). To investigate the potential role of miRNAs in the post-transcriptional regulation of *HCN2* and *HCN4* genes, we measured the expression level of miR-1, miR-133a and miR-133b, which are specifically expressed in normal adult heart. Results of qRT-PCR showed no changes in post-MI rats, while a significant increase in miR-1, miR-133a,

Table 1

Properties of I_{K1} in myocytes from LV, LA and RV myocytes isolated from post-MI rats receiving ivabradine (10 mg·kg^{-1}·day^{-1}) (MI + IVA) or vehicle (MI) for 3 months and sham-operated rats

	Sham (n = 5–6 rats) (12–13 cells)	MI (5–8 rats) (9–15 cells)	MI + IVA (n = 5–8 rats) (12–13 cells)
LV myocytes			
I_{K1} density at –100 mV (pA/pF)	–4.7 ± 1.1	–6.8 ± 1.6	–6.0 ± 1.1
I_{K1} density at –55 mV (pA/pF)	0.3 ± 0.2	0.5 ± 0.1	0.4 ± 0.1
Reversal potential (mV)	–65.6 ± 0.1	–66.6 ± 0.1	–67.3 ± 0.1
LA myocytes			
I_{K1} density at –100 mV (pA/pF)	–9.8 ± 2.2	–8.2 ± 1.8	–7.6 ± 1.9
I_{K1} density at –55 mV (pA/pF)	0.5 ± 0.1	0.3 ± 0.1	0.5 ± 0.2
Reversal potential (mV)	–62.8 ± 0.1	–63.8 ± 0.1	–64.9 ± 0.1
RV myocytes			
I_{K1} density at –100 mV (pA/pF)	–7.8 ± 1.6	–8.5 ± 1.7	–9.2 ± 1.4
I_{K1} density at –55 mV (pA/pF)	0.7 ± 0.1	0.8 ± 0.2	1.0 ± 0.1
I_{K1} potential (mV)	–69.7 ± 0.1	–69.8 ± 0.1	–68.9 ± 0.1

I_{K1}, inward rectifier current; LV, left ventricular; LA, left atrial; RV, right ventricular; MI, myocardial infarction.

and miR-133b occurred in ventricles from the MI + IVA rats versus sham and MI rats (n = 6 for all groups) (miR-1: 1.84 ± 0.22 vs. 1.06 ± 0.16 and 0.96 ± 0.12; miR-133a: 1.55 ± 0.03 vs. 1.03 ± 0.11 and 1.09 ± 0.16; miR-133b: 2.5 ± 0.4 vs. 1.03 ± 0.12 and 1.09 ± 0.13; $P < 0.05$) (Figure 5A). In atrial tissue we observed a significant increase in miR-1 from MI + IVA rats (3.76 ± 1.09) versus sham (1.09 ± 0.2) and MI rats (0.59 ± 0.01, $P < 0.05$) (Figure 5B). Moreover, miR-1 tends to decrease in LA from MI versus sham rats (NS).

Discussion

Our results show that induction of MI using LAD ligation significantly increased I_f specific conductance by 144% in LV myocytes ($P < 0.01$) and 218% in LA myocytes ($P < 0.05$), as was expected from our previous studies (Sartiani *et al.*, 2006). Ivabradine partially reverses the electrophysiological remodelling occurring in post-MI rats, and I_f specific conductance was reduced by 30% and 28% in the LV and LA myocytes, respectively. Similar effects were observed in RV myocytes. The effects of ivabradine on electrophysiological remodelling were accompanied by a down-regulation in overexpression of mRNA coding for *HCN2* and/or *HCN4* in LV and RV tissue, although with a different regional distribution. Therefore, especially at the ventricular level, our results show a good correlation between functional and molecular data, particularly between sham and MI rats. As for the treated MI rats, mRNA levels showed regional differences, whereas current specific conductance or occurrence was almost homogeneously reduced in LV, LA, and RV myocytes. In particular, values for *HCN2* (LV) and *HCN4* (LA) were significantly higher than in sham, but microRNA miR-1 and miR-133, which modulate post-transcriptional repression of *HCN2* and *HCN4* genes (Xiao *et al.*, 2007), were significantly increased in LV myocytes from MI+IVA. These findings are consistent with the potential benefits of ivabradine on cardiac function via the reversal of electrophysiological remodelling due to transcriptional and post-transcriptional mechanisms.

Cardiac electrophysiological remodelling is a complex phenomenon that accompanies the global remodelling of the diseased heart. Several characteristics are changed in the expression and function of specific ionic conductances. In line with previous observations (Sartiani *et al.*, 2006), I_f gain-of-function is detected in ventricular myocytes from post-MI rat hearts. Our recently published data show an increased action potential duration (APD) associated with a reduction in transient outward current (I_{to}) in post-MI rats hearts (Ceconi *et al.*, 2011). It has been suggested that these changes are reminiscent of the immature myocytic phenotype, characterized by a prolonged APD, increased I_f occurrence and density, and decreased I_{to} density (Cerbai *et al.*, 1999).

In agreement with previous data obtained in rat models of LV hypertrophy (Fernandez-Velasco *et al.*, 2003) and human samples from explanted hearts (Stillitano *et al.*, 2008), our results indicate that increased functional overexpression of I_f in cardiomyopathy may be largely attributable to transcriptional mechanisms, because it was associated with a significant increase in mRNA for both *HCN2* and *HCN4* isoforms in LV tissue from post-MI rats. Although a qualitative comparison of I_f conductance was prevented by low current density, higher current occurrence and *HCN4* expression in the RV of MI rats also suggests that electrophysiological remodelling occurs in an area distant from the scar. This result is in line with data obtained in the same model (Sartiani *et al.*, 2006; Tavares *et al.*, 2007) and may reflect pulmonary hypertension in response to increased LV filling pressure and/or circulating hypertrophic stimuli.

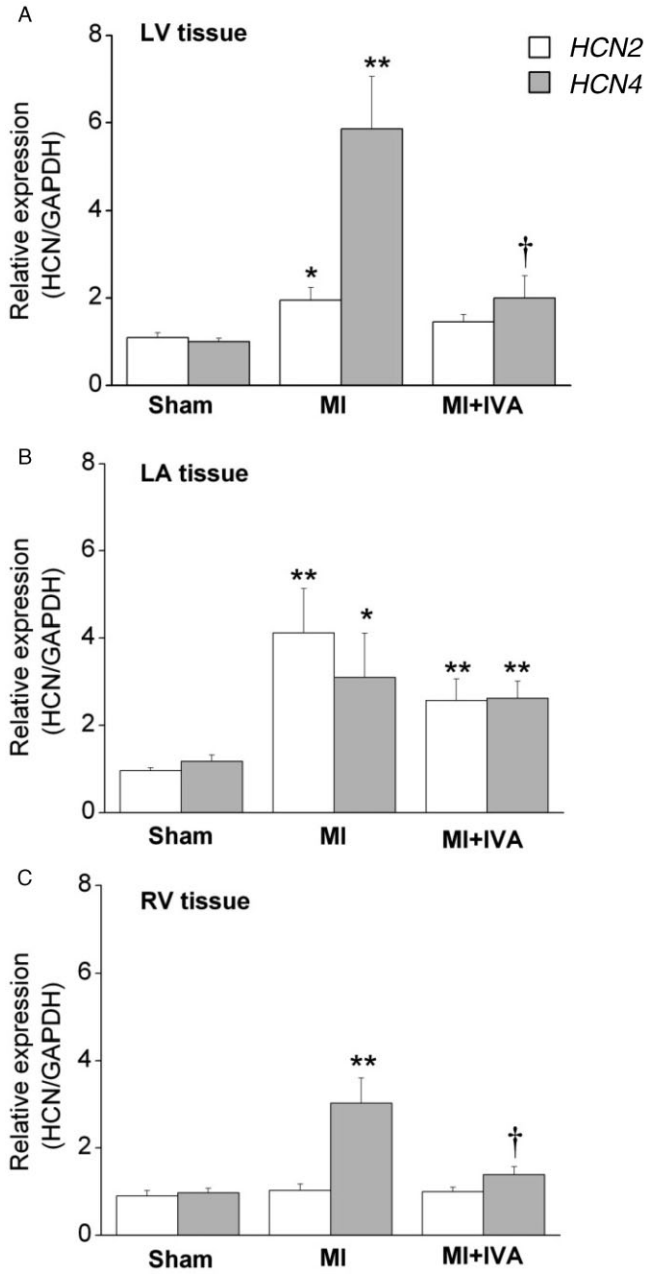

Figure 4

Relative expression of *HCN2* and *HCN4* normalized to GAPDH in left ventricular (LV), left atrial (LA) and right ventricular (RV) tissue samples from post-myocardial infarcted rats receiving ivabradine (10 mg·kg^{-1}·day^{-1} in drinking water) for 3 months (MI + IVA, $n = 5$ or 6 samples), post-myocardial infarcted rats (MI, $n = 4$–7 samples) and sham-operated animals (sham, $n = 5$–7 samples) receiving vehicle for 3 months. RV data are averages of four to six samples. *$P < 0.05$, **$P < 0.01$ versus sham rats; †$P < 0.05$ versus MI rats. MI, myocardial infarction.

Interestingly, the regulation of *HCN2* and *HCN4* expression seems to differ between the ventricle and the atrium, suggesting region-specific increases in expression after myocardial injury. The reasons for regional differences remain

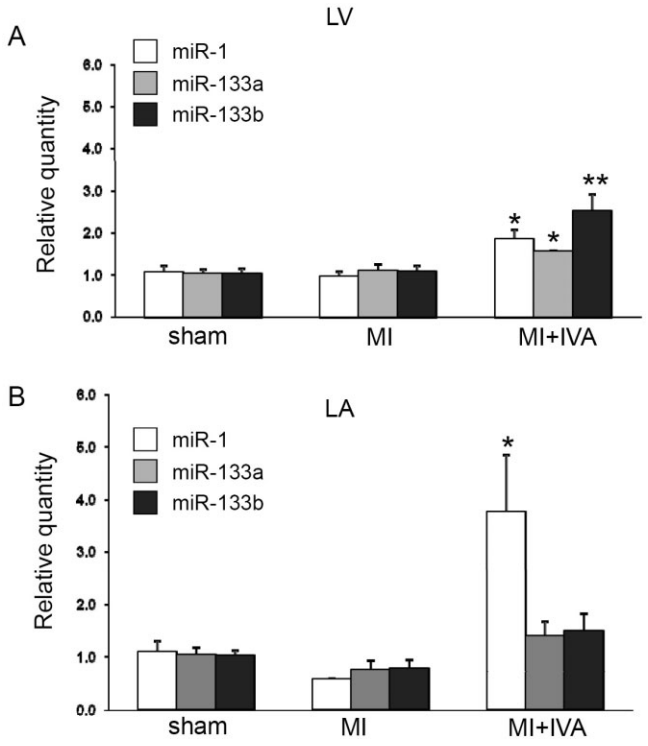

Figure 5

Relative expression of miR-1 and miR-133a/b in left ventricular (A) and atrial (B) tissue from post-myocardial infarcted rats (MI), and post-myocardial infarcted rats treated with ivabradine (MI + IVA), and sham-operated animals (Sham) by TaqMan-qRT-PCR. Each column represents the mean of six different samples in triplicate ± SEM. *$P < 0.05$, **$P < 0.01$ versus sham and MI rats. MI, myocardial infarction; LA, left atrial tissue; LV, left ventricular tissue.

unclear, partly because the factors involved in the HCN transcription mechanisms are not yet well understood.

Treatment with ivabradine models I_f function in the post-MI atrial and ventricular tissue partially counteracting the up-regulation of I_f associated with cardiac disease in our experiments. These results were not entirely anticipated for several reasons. Firstly, any agent that involves electrophysiological blockade may also affect the trafficking of target or non-target proteins (van der Heyden *et al.*, 2008), leading to unexpected effects in terms of up-regulation or down-regulation of the current involved. Secondly, long-term treatment with ivabradine has been reported to up-regulate mRNA levels in healthy mouse sinoatrial node, but not in the ventricle (Leoni *et al.*, 2005); however, at variance with rat and human hearts, I_f expression is hardly detectable in adult mouse ventricle either in normal or diseased hearts (Yasui *et al.*, 2001).

Overall, our data from the post-MI rat model suggest that I_f up-regulation mainly depends on transcriptional mechanisms, for example *HCN2* and *HCN4* overexpression clearly evident in our experimental conditions. Thus, in this respect, the post-MI rat behaves similarly to human terminal ischaemic cardiomyopathy (Stillitano *et al.*, 2008).

Our results demonstrate that, in the LV of MI + IVA rats, *HCN4* mRNA levels returned to values similar to those mea-

sured in sham, and significantly lower than those measured in MI rats; the same holds true for the RV. Most likely, this result cannot be attributed to a direct effect of ivabradine: in sham rats, ivabradine treatment, while decreasing HR, does not decrease I_f or *HCN2*/*HCN4* levels; a small yet significant increase in *HCN2* (for the LV only) was observed. We conclude that HR reduction by ivabradine counteracts electrophysiological maladaptive remodelling only in a pathological setting, such as MI, which induces I_f gain-of-function.

In the LA, however, *HCN2* and *HCN4* mRNA levels in MI + IVA remained significantly higher than in sham, even though the decrease in current conductance was similar to the LV. A different transcription profile in HCN isoforms among cardiac chambers occurs throughout fetal and postnatal development in mice (Schweizer *et al*., 2009). Notwithstanding differences in species and experimental model, these observations seem to indicate a region-specific control of HCN isotypes, the basis of which remains to be elucidated. The discrepancy between mRNA levels and current density, however, prompted us to investigate the contribution of post-transcriptional mechanisms.

Post-transcriptional regulation of these genes has been recently demonstrated; in particular, data in hypertrophic hearts induced by aortic stenosis indicate that microRNA miR-1/miR-133 may contribute to the overexpression of the pacemaker HCN channels (Luo *et al*., 2008). In our experimental conditions, miR-1/miR-133 expression did not change in post-MI rats versus sham. This could be explained by the fact that miR-1 plays a role in the induction of hypertrophy throughout the initial phase of cardiac growth. Indeed, it has been demonstrated that miR-1 is down-regulated as early as 1 day after thoracic aortic constriction, while it appears to return to normal levels after 14 days; miR-133a/b, which is also highly expressed in the heart, remained unchanged up to 14 days after thoracic aortic constriction (Sayed *et al*., 2007). By contrast, in a mouse model of MI, miR-133a was significantly down-regulated 7 days after coronary artery ligation and recovered afterwards (van Rooij *et al*., 2008).

Interestingly, we found that miR-1 and miR-133a/b are up-regulated during reverse remodelling consequent to ivabradine treatment. Recent studies show that miR-1 modulates post-transcriptionally both *HCN2* and *HCN4* (Xiao *et al*., 2007) and may contribute to overexpression of pacemaker channels in cardiac hypertrophy (Luo *et al*., 2008). miR-133a and miR-1 are encoded by the same pre-miRNA, and can suppress channel protein expression by promoting mRNA degradation or by repressing protein translation (Chen *et al*., 2006). Indeed, decreased miR-1 and miR-133 levels have been associated with increased I_f expression in animal models of HF (Luo *et al*., 2008). In our study, we did not observe a down-regulation in MI rats; this is in agreement with previous results showing that miR-1 levels are transiently modulated after MI and return to basal values afterwards (D'Alessandra *et al*., 2010). However, in ivabradine-treated MI rats, miR-1 was significantly increased in LV and LA specimens with respect to untreated MI rats. miR-133 was also increased in LV, but not in LA, although the reason for this discrepancy is at present unclear and deserves further investigation. Notwithstanding regional differences, overexpression of miRNA in MI + IVA rats is suggestive of a post-transcriptional repression of *HCN2* and *HCN4*, which may contribute to reduced functional expression of I_f in these rats. Besides HCN genes, miR-1 and miR-133 have been associated with several target channels as targets in the setting of myocardial remodelling, such as ventricular hypertrophy or atrial fibrillation (Luo *et al*., 2010); therefore, the effect of ivabradine on the miR profile deserves further investigation.

Limitations of the study

Although a significant lowering of HR was detected in MI + IVA rats (present results; Ceconi *et al*., 2011), our study cannot rule out the possibility that reverse remodelling during ivabradine treatment occurs, at least in part, by mechanisms beyond HR reduction (Heusch, 2008). In this respect, recent data by Christensen *et al*. (2009) also show advantages of ivabradine over atenolol despite similar bradycardic action. As speculated elsewhere (Terracciano and Yacoub, 2010), ivabradine blockade of (residual) f-current may also affect directly electrogenesis in failing atrial or ventricular myocytes. However, a direct contribution of I_f to normal or abnormal electrogenesis in non-pacemaker cells cannot be inferred at present. Finally, a limitation of our study is that transmural differences in the effects of ivabradine on HCN expression could not be evaluated because the ventricular samples contained epicardial, midmyocardial and endocardial cells. This is important because it has been established that electrical heterogeneity occurs within the human ventricular wall, possibly due to the differential expression of ion channel genes (Antzelevitch and Fish, 2001). On the other hand, transcription of HCN isoforms has been reported not to vary within the LV wall in healthy rat or canine hearts (Rosati *et al*., 2006).

Conclusion

Our results show that chronic HR reduction with ivabradine partially reverses electrophysiological cardiac remodelling in post-MI rats by reducing I_f gain-of-function. This is attributable to transcriptional and post-transcriptional mechanisms. Although the electrogenic and/or pro-arrhythmic role of this current in the working myocardium remains elusive, I_f gain-of-function may be considered a hallmark of atrial and ventricular remodelling in cardiac hypertrophy and failure.

Thus, in addition to previous results showing a beneficial biochemical remodelling (Dedkov *et al*., 2007; Christensen *et al*., 2009; Milliez *et al*., 2009; Ceconi *et al*., 2011), our new results provide further support for a cardioprotective effect of ivabradine in ischaemic heart disease.

Acknowledgements

We wish to thank CeSAL personnel for technical support in animal care. This work was supported by research grants from Servier S.p.A., Ministero Istruzione Università e Ricerca (PRIN2007 and 2008), European Union (LSH M/CT/2006/018676 to E.C.) and Ente Cassa di Risparmio di Firenze.

Conflicts of interest

Alessandro Mugelli and Claudio Ceconi have served as speakers for Servier, and have received research grants from Servier; Roberto Ferrari has received consultancy fees, research grants and payment service for speakers' bureau from Servier; Muriel Bouly is an employee of the Institut de Recherches Internationales Servier. Silvia Suffredini, Francesca Stillitano, Simona Brogioni, Laura Comini and Elisabetta Cerbai have no conflict of interest.

References

Antzelevitch C, Fish J (2001). Electrical heterogeneity within the ventricular wall. Basic Res Cardiol 96: 517–527.

Böhm M, Swedberg K, Komajda M, Borer JS, Ford I, Dubost-Brama A *et al.* (2010). Heart rate as a risk factor in chronic heart failure (SHIfT): the association between heart rate and outcomes in a randomised placebo-controlled trial. Lancet 376: 886–894.

Ceconi C, Comini L, Suffredini S, Stillitano F, Bouly M, Cerbai E *et al.* (2011). Heart rate reduction with ivabradine prevents the global phenotype of left ventricular remodeling. Am J Physiol Heart Circ Physiol 300: H366–H373.

Cerbai E, Barbieri M, Mugelli A (1996). Occurrence and properties of the hyperpolarization-activated current I(f) in ventricular myocytes from normotensive and hypertensive rats during aging. Circulation 94: 1674–1681.

Cerbai E, Pino R, Porciatti F, Sani G, Toscano M, Maccherini M *et al.* (1997). Characterization of the hyperpolarization-activated current, I(f), in ventricular myocytes from human failing heart. Circulation 95: 568–571.

Cerbai E, Pino R, Sartiani L, Mugelli A (1999). Influence of postnatal-development on I(f) occurrence and properties in neonatal rat ventricular myocytes. Cardiovasc Res 42: 416–423.

Cerbai E, Sartiani L, DePaoli P, Pino R, Maccherini M, Bizzarri F *et al.* (2001). The properties of the pacemaker current I(f) in human ventricular myocytes are modulated by cardiac disease. J Mol Cell Cardiol 33: 441–448.

Chen JF, Mandel EM, Thomson JM, Wu Q, Callis TE, Hammond SM *et al.* (2006). The role of microRNA-1 and microRNA-133 in skeletal muscle proliferation and differentiation. Nat Genet 38: 228–233.

Christensen LP, Zhang RL, Zheng W, Campanelli JJ, Dedkov EI, Weiss RM *et al.* (2009). Postmyocardial infarction remodeling and coronary reserve: effects of ivabradine and beta blockade therapy. Am J Physiol Heart Circ Physiol 297: H322–H330.

D'Alessandra Y, Devanna P, Limana F, Straino S, Di Carlo A, Brambilla PG *et al.* (2010). Circulating microRNAs are new and sensitive biomarkers of myocardial infarction. Eur Heart J 31: 2765–2773.

Dedkov EI, Zheng W, Christensen LP, Weiss RM, Mahlberg-Gaudin F, Tomanek RJ (2007). Preservation of coronary reserve by ivabradine-induced reduction in heart rate in infarcted rats is associated with decrease in perivascular collagen. Am J Physiol Heart Circ Physiol 293: H590–H598.

DiFrancesco D (2006). Serious workings of the funny current. Prog Biophys Mol Biol 90: 13–25.

Fernandez-Velasco M, Goren N, Benito G, Blanco-Rivero J, Bosca L, Delgado C (2003). Regional distribution of hyperpolarization-activated current (If) and hyperpolarization-activated cyclic nucleotide-gated channel mRNA expression in ventricular cells from control and hypertrophied rat hearts. J Physiol 553: 395–405.

Heusch G (2008). Pleiotropic action(s) of the bradycardic agent ivabradine: cardiovascular protection beyond heart rate reduction. Br J Pharmacol 155: 970–971.

van der Heyden MA, Smits ME, Vos MA (2008). Drugs and trafficking of ion channels: a new pro-arrhythmic threat on the horizon? Br J Pharmacol 153: 406–409.

Hoppe UC, Beuckelmann DJ (1998). Characterization of the hyperpolarization-activated inward current in isolated human atrial myocytes. Cardiovasc Res 38: 788–801.

Leoni AL, Marionneau C, Demolombe S, Le BS, Mangoni ME, Escande D *et al.* (2005). Chronic heart rate reduction remodels ion channel transcripts in the mouse sinoatrial node but not in the ventricle. Physiol Genomics 24: 4–12.

Liu J, Dobrzynski H, Yanni J, Boyett MR, Lei M (2007). Organisation of the mouse sinoatrial node: structure and expression of HCN channels. Cardiovasc Res 73: 729–738.

Livak KJ, Schmittgen TD (2001). Analysis of relative gene expression data using real-time quantitative PCR and the 2(-Delta Delta C(T)) method. Methods 25: 402–408.

Luo X, Lin H, Pan Z, Xiao J, Zhang Y, Lu Y *et al.* (2008). Down-regulation of miR-1/miR-133 contributes to re-expression of pacemaker channel genes HCN2 and HCN4 in hypertrophic heart. J Biol Chem 283: 20045–20052.

Luo X, Zhang H, Xiao J, Wang Z (2010). Regulation of human cardiac ion channel genes by microRNAs: theoretical perspective and pathophysiological implications. Cell Physiol Biochem 25: 571–586.

Milliez P, Messaoudi S, Nehme J, Rodriguez C, Samuel JL, Delcayre C (2009). Beneficial effects of delayed ivabradine treatment on cardiac anatomical and electrical remodeling in rat severe chronic heart failure. Am J Physiol Heart Circ Physiol 296: H435–H441.

Mulder P, Barbier S, Chagraoui A, Richard V, Henry JP, Lallemand F *et al.* (2004). Long-term heart rate reduction induced by the selective I(f) current inhibitor ivabradine improves left ventricular function and intrinsic myocardial structure in congestive heart failure. Circulation 109: 1674–1679.

van Rooij E, Sutherland LB, Thatcher JE, DiMaio JM, Naseem RH, Marshall WS *et al.* (2008). Dysregulation of microRNAs after myocardial infarction reveals a role of miR-29 in cardiac fibrosis. Proc Natl Acad Sci USA 105: 13027–13032.

Rosati B, Grau F, McKinnon D (2006). Regional variation in mRNA transcript abundance within the ventricular wall. J Mol Cell Cardiol 40: 295–302.

Sartiani L, De Paoli P, Stillitano F, Aimond F, Vassort G, Mugelli A *et al.* (2006). Functional remodeling in post-myocardial infarcted rats: focus on beta-adrenoceptor subtypes. J Mol Cell Cardiol 40: 258–266.

Sayed D, Hong C, Chen IY, Lypowy J, Abdellatif M (2007). MicroRNAs play an essential role in the development of cardiac hypertrophy. Circ Res 100: 416–424.

Schweizer PA, Yampolsky P, Malik R, Thomas D, Zehelein J, Katus HA *et al*. (2009). Transcription profiling of HCN-channel isotypes throughout mouse cardiac development. Basic Res Cardiol 104: 621–629.

Stillitano F, Lonardo G, Zicha S, Varro A, Cerbai E, Mugelli A *et al*. (2008). Molecular basis of funny current (If) in normal and failing human heart. J Mol Cell Cardiol 45: 289–299.

Swedberg K, Komajda M, Böhm M, Borer JS, Ford I, Dubost-Brama A *et al*. (2010). Ivabradine and outcomes in chronic heart failure (SH*I*$_f$T): a randomised placebo-controlled study. Lancet 376: 875–885.

Tavares NI, Philip-Couderc P, Papageorgiou I, Baertschi AJ, Lercha R, Montessuit R (2007). Expression and function of ATP-dependent potassium channels in late post-infarction remodeling. J Mol Cell Cardiol 42: 1016–1025.

Teerlink JR (2010). Ivabradine in heart failure – no paradigm SH*I*$_f$T . . . yet. Lancet 376: 847–849.

Terracciano CM, Yacoub MH (2010). Heart failure: a SH*I*$_f$T from ion channels to clinical practice. Nat Rev Cardiol 7: 669–670.

Xiao J, Yang B, Lin H, Lu Y, Luo X, Wang Z (2007). Novel approaches for gene-specific interference via manipulating actions of microRNAs: examination on the pacemaker channel genes HCN2 and HCN4. J Cell Physiol 212: 285–292.

Yasui K, Liu W, Opthof T, Kada K, Lee JK, Kamiya K *et al*. (2001). I(f) current and spontaneous activity in mouse embryonic ventricular myocytes. Circ Res 88: 536–542.